

The ELAIS Deep X-ray Survey

C.J. Willott

Astrophysics, University of Oxford, Keble Road, Oxford OX1 3RH, U.K.

O. Almaini, J. Manners, O. Johnson, A. Lawrence, J.S. Dunlop, R.G. Mann

Institute for Astronomy, University of Edinburgh, Blackford Hill, Edinburgh EH9 3HJ, U.K.

I. Perez-Fournon, E. Gonzalez-Solares, F. Cabrera-Guerra

Instituto de Astrofísica de Canarias, C/ Via Lactea s/n, 38200 La Laguna, Tenerife, Spain

S. Serjeant

Unit for Space Sciences and Astrophysics, The University of Kent, Canterbury, Kent CT2 7NR, UK

S.J. Oliver

Astronomy Centre, CPES, University of Sussex, Falmer, Brighton, Sussex BN1 9QJ, UK

M. Rowan-Robinson

Astrophysics Group, Blackett Laboratory, Imperial College of Science Technology & Medicine (ICSTM), Prince Consort Rd, London SW7 2BZ, UK

We present initial follow-up results of the ELAIS Deep X-ray Survey which is being undertaken with the Chandra and XMM-Newton Observatories. 235 X-ray sources are detected in our two 75 ks ACIS-I observations in the well-studied ELAIS N1 and N2 areas. 90% of the X-ray sources are identified optically to $R = 26$ with a median magnitude of $R = 24$. We show that objects which are unresolved optically (i.e. quasars) follow a correlation between their optical and X-ray fluxes, whereas galaxies do not. We also find that the quasars with fainter optical counterparts have harder X-ray spectra, consistent with absorption at both wavebands. Initial spectroscopic follow-up has revealed a large fraction of high-luminosity Type 2 quasars. The prospects for studying the evolution of the host galaxies of X-ray selected Type 2 AGN are considered.

1 Introduction

X-ray astronomy is moving into a new era with the successful launch of the Chandra and XMM-Newton observatories. The combination of large collecting area, high spatial resolution and wide spectral range enable new surveys to probe deeper than ever before and resolve most of the hard X-ray (2-10 keV) background (XRB). The peak intensity of the XRB lies at 30 keV and models of the XRB spectrum (e.g. Comastri et al. 1995; Gilli et al. 1999) predict that obscured AGN with very hard spectra must be much more common in the Universe than naked quasars. Ordinary, optically selected AGN perhaps account for only 10-20% of the total hard XRB. The direct implication is that most of the accretion activity in the Universe is absorbed.

We are conducting a deep X-ray survey with Chandra and XMM-Newton in fields which have been well-studied at other wavebands. In each of the two fields, designated N1 and N2,

Chandra ACIS-I observations of duration 75 ks have been made. A total of 235 X-ray sources are detected in the full band images above a flux limit of $S_{0.5-10\text{keV}} > 1.3 \times 10^{-15} \text{ erg cm}^{-2} \text{ s}^{-1}$. We have also been awarded time for a 150 ks observation of N2 with XMM-Newton. Multi-wavelength coverage is very important for understanding the nature of the X-ray sources. Our fields lie within the European Large-Area ISO Survey (ELAIS) and have been observed with ISO at 7, 15, 90 and 175 μm (Oliver et al. 2000) and with the VLA at 1.4 GHz (Ciliegi et al. 1999). One of the two X-ray fields is co-incident with the widest survey yet made with SCUBA on the JCMT – the UK Submillimetre Consortium’s 8 mJy Survey (Dunlop et al. 2000).

The goals of our survey are to obtain a better understanding of the nature of the AGN responsible for the X-ray background (or equivalently, the accretion history of the Universe) and the host galaxies they reside in. Some of the questions to be answered are: What is the connection between AGN activity and star-formation? Do X-ray AGN live in old, evolved galaxies or young galaxies with high levels of star-formation? What are the clustering properties of X-ray sources, both with other X-ray sources and with the general galaxy population? How much of the accretion energy of the Universe is obscured and reprocessed by dust? Is the dust distribution well-represented by torus models with typical galactic gas-to-dust ratios? What X-ray luminosity dependence is there on host galaxy/torus properties? The answers to these questions will come from detailed follow-up of deep X-ray surveys.

Note that the small sky areas covered in each pointing with Chandra (equivalent to $\sim 7 \times 7$ Mpc at $z \gtrsim 1$) mean that the effects of small-scale clustering and cosmic variance are important. For example, in the N1 field the density of X-ray sources brighter than a given flux-limit is approximately 30% higher than that in N2. Thus, no single ultradeep survey (such as the Chandra Deep Field South or the Hubble Deep Field North) will be able to accurately determine the contribution to the XRB, the redshift distribution or luminosity function of X-ray AGN. Only by combining the results of several deep surveys will such results be obtainable.

A flat cosmology with parameters $H_0 = 70 \text{ km s}^{-1} \text{ Mpc}^{-1}$, $\Omega_M = 0.3$ and $\Omega_\Lambda = 0.7$ is assumed throughout.

2 Optical Identification of the ELAIS Deep X-ray Survey

Optical imaging data covering the Chandra fields has been obtained with the William Herschel Telescope (WHT) Prime-Focus Camera and the Isaac Newton Telescope (INT) Wide-Field Camera. The WHT data are only in N2 and reach to limiting Vega magnitudes of $R \approx 26$ and $I \approx 26$. INT data in both fields reach limiting AB magnitudes of $g' \approx 25.5$, $r' \approx 25$, $i' \approx 24.5$. In the near-infrared there is full coverage of both fields at H -band with CIRS on the INT and partial K -band coverage from INGRID on the WHT and UFTI on the UKIRT. Full details of all these observations will be presented in forthcoming papers.

For initial identification of the X-ray sources detected in the full (0.5-10 keV) band, we consider only the WHT R -band imaging in N2 and the INT r' -band imaging in N1. The X-ray and optical astrometric frames are registered using ≈ 20 X-ray sources which are optically bright. The adopted identification procedure takes into account the positional uncertainty of the Chandra source, which is dependent upon the number of photons detected and the off-axis angle (since the PSF is degraded as one moves further from the centre of the field). The positional uncertainties range from 0.5 to 2.5 arcsec. A modified version of the likelihood ratio procedure (Sutherland & Saunders 1992) was used to determine the likelihood of possible identifications. Full details of the adopted method will be given in Gonzalez-Solares et al. (in prep.). The median magnitude of the X-ray source counterparts is $R \approx 24$ with 90% identified to a limit of $R = 26$. Our results show a small, but non-negligible, percentage of chance associations (5%) of optical counterparts to Chandra sources, most of which would occur near the field edges where the Chandra PSF is quite large. Note that this will be a serious problem for deep XMM-

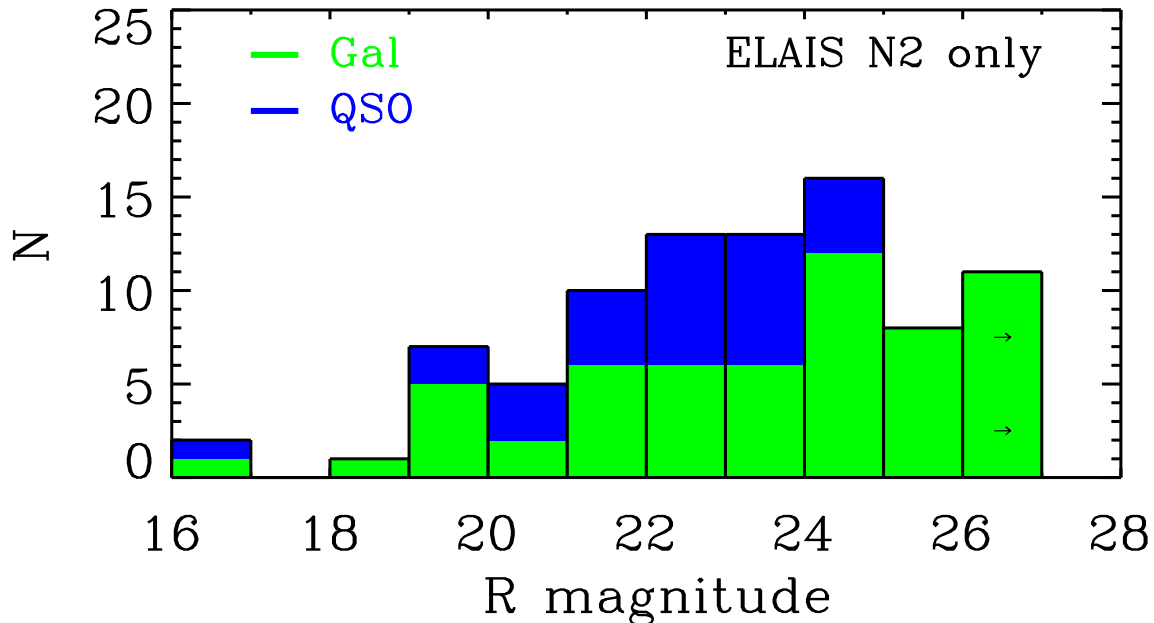


Figure 1: Magnitude histogram of Chandra source optical identifications in the ELAIS N2 region. The histogram is split into those objects with a quasar-like unresolved optical appearance and those which appear to be galaxies.

Newton surveys which have lower spatial resolution than Chandra. Combining XMM-Newton and Chandra data will help to alleviate this problem.

The good seeing (0.8 arcsec) of the optical imaging allows us to make a morphological classification of the optical counterparts of X-ray sources. We have used the SExtractor program to generate image source catalogues and the parameter CLASS_STAR is used to determine whether an object has an unresolved (stellar) or resolved (galaxy) morphology. The unresolved sources correspond predominantly to quasars in which the light from the active nucleus substantially outshines that of its host galaxy, whereas the resolved counterparts will be dominated by starlight with any AGN component absorbed or intrinsically weak. In Figure 1 we show a histogram of the magnitudes of X-ray source identifications in the N2 region, for which the star-galaxy separation works well down to $R = 25$. There are approximately equal numbers of quasars and galaxies at magnitudes brighter than $R = 24$ and then galaxies begin to dominate at fainter magnitudes. We note that our results appear inconsistent with those of Giacconi et al. (2001) who quote that two-thirds of the counterparts to Chandra sources in the Chandra Deep Field South (CDFS) appear point-like. However, high-resolution studies with the HST of a subset of the CDFS sources (Schreier et al. 2001), shows an unresolved fraction of about one third, similar to that in Fig.1.

Figure 2 plots the X-ray flux of sources against their optical magnitudes. The quasars clearly show a well-defined correlation with most sources lying in the band $1 < L_X/L_{\text{opt}} < 10$. This correlation is similar to that found for soft X-ray selected quasars (Hasinger et al. 1999). We note that at least one of the few ‘quasar’ objects to the left of this diagram is spectroscopically confirmed as a star. In contrast to the quasars, the distribution of galaxies on this plot is much less well-defined. This is because for the galaxies, the optical light is dominated by the stellar population, which is not tightly correlated with the X-ray flux coming, presumably, from the nucleus. There are many galaxies with $L_X/L_{\text{opt}} > 10$, which are presumably Type-2 quasars in which the optical flux is much more readily depressed by absorption than the hard X-rays.

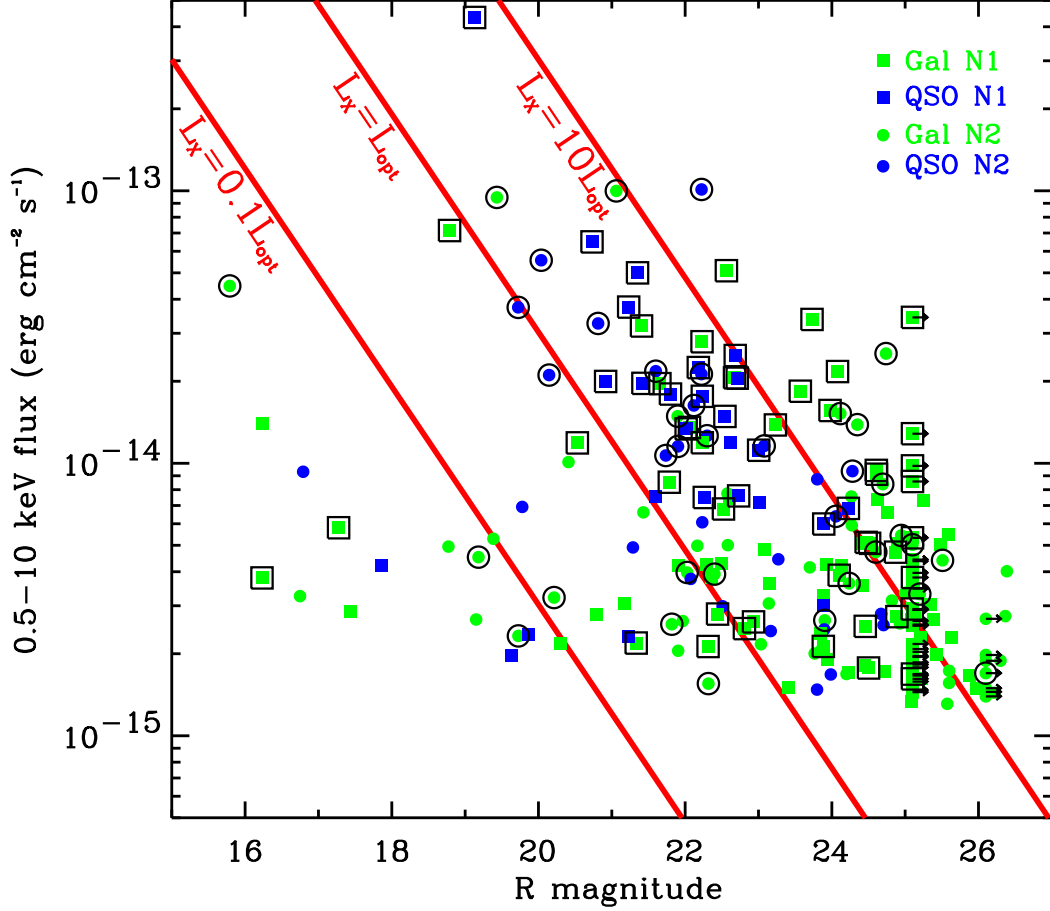


Figure 2: 0.5-10 keV flux against R magnitude for ELAIS Chandra sources. Sources also detected in the hard band images (2-10 keV) are shown as symbols with a black border.

The correlation between optical and X-ray flux exhibited by the quasars, but not the galaxies, explains why the fraction of galaxy counterparts increases fainter than $R = 24$, since it is at this magnitude where $L_X \approx L_{\text{opt}}$ at our X-ray flux limit.

3 Comparison of optical properties with X-ray hardness

An analysis of the hardness ratios, $HR = [(H - S)/(H + S)]$, of the Chandra sources shows that HR increases at fainter fluxes (as seen in the CDFS – Tozzi et al. 2001). The simplest explanation of this effect is that sources get harder at lower luminosities, since the redshift distribution is unlikely to change significantly from 10^{-14} to 10^{-15} erg cm $^{-2}$ s $^{-1}$. It is worth pointing out that HR alone is not a good measure of the absorption of an absorbed power-law X-ray source. Due to the negative k-correction of a highly absorbed source, sources at high redshift will have much lower values of HR than sources with the same rest-frame spectra at lower redshifts. In Figure 3 we plot the hardness ratio HR against the R magnitude. Note that the hardest sources are galaxies, indicating a lack of quasars with hard spectra. Many of the hard ($HR > 0$) galaxies are very faint, which suggests they are at high redshifts ($z > 1$) and have large absorbing columns. There is no overall correlation of HR with magnitude for the galaxies, although this non-correlation is not trivial to interpret given the positive correlation between R and z for galaxies and the negative correlation between HR and z for a given absorbing column. This could be indicating a more rapid evolution of hard sources than soft sources, as required

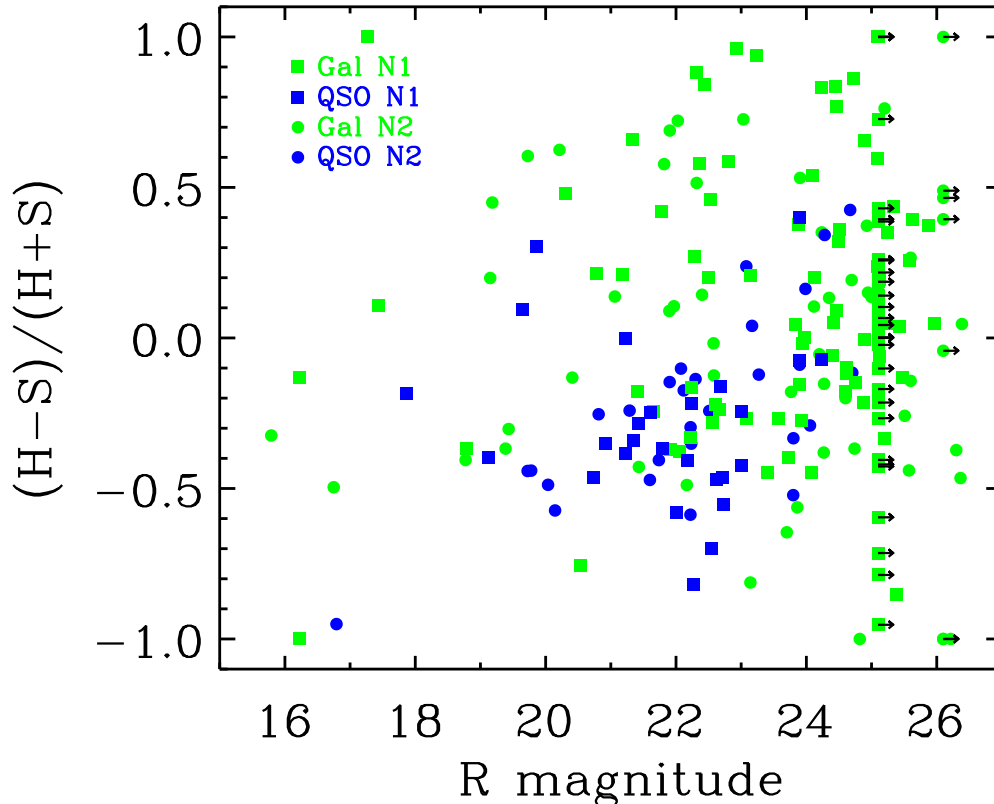


Figure 3: Hardness ratio against optical magnitude for ELAIS Chandra sources.

by some XRB models (e.g. Gilli et al. 2001).

The hardness ratio of an unabsorbed, broad line quasar is typically $HR = -0.5$. Most of the optically bright quasars ($R < 23$) in Fig. 3 show values similar to this. However, the fainter quasars tend to have harder X-ray spectra such that at $R = 24$, $HR \approx 0$. This cannot be a redshift effect because HR decreases at high redshift and if these sources were at low redshift then their galaxies would outshine the nucleus in the optical. A simple explanation for this change is that some of the optically fainter quasars are undergoing absorption in their environments, both in the optical by dust and in the X-rays by cool gas. The nuclear region in such sources may suffer a few magnitudes of extinction or may be totally obscured, in which case the light we observe is either scattered into our line-of-sight or emitted from a region beyond the obscuring medium. For a galactic gas-to-dust ratio, the large absorbing columns necessary for such hard X-ray spectra would equate to very high optical reddening, suggesting that either the light we observe is scattered or there is a very high gas-to-dust ratio as found in some low-redshift Seyferts (Maiolino et al. 2001).

4 The fraction of high-luminosity Type 2 quasars

Models of the X-ray background have long postulated the existence of high-luminosity ($L_{2-10\text{keV}} > 10^{44}\text{erg cm}^{-2} \text{ s}^{-1}$), obscured Type 2 quasars, showing only narrow emission lines. Within the unified scheme for AGN, it is expected that the central regions of Type 2 quasars are obscured along our line-of-sight by a dusty torus (e.g. Antonucci 1993). However, previous hard X-ray

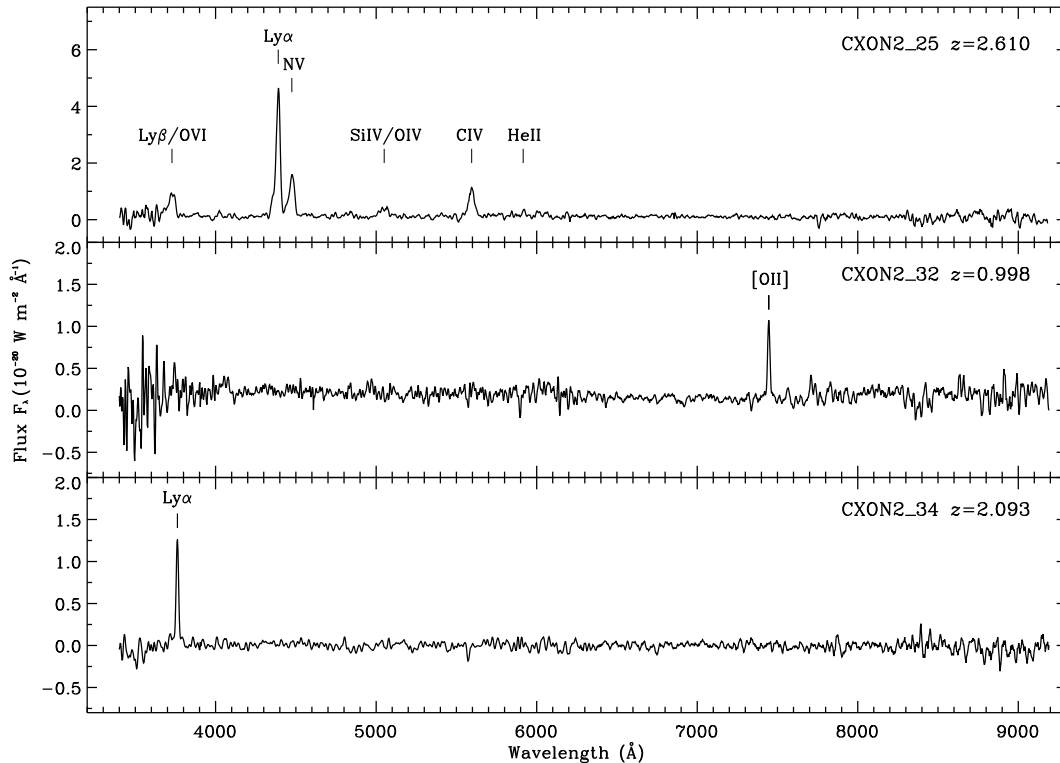


Figure 4: Optical spectra of hard X-ray selected ELAIS Chandra sources. The sources are radio-quiet Type 2 quasars.

surveys with ASCA and BeppoSax have revealed few such objects leading some authors to doubt their existence at all (Halpern et al. 1999).

Of course, radio-loud Type 2 quasars (i.e. radio galaxies) have been known for a long time and it is worth considering the known properties of high-redshift radio galaxies when searching for similar objects which are radio-quiet. The ratio of narrow-line to broad-line high-luminosity radio-loud AGN is well determined by virtue of the isotropy of extended low-frequency radio emission and is 1.5 (Barthel 1989). At lower radio luminosities (151MHz luminosities $L_{151} < 3 \times 10^{26} \text{ W Hz}^{-1} \text{ sr}^{-1}$) this ratio increases to ≈ 7 (Willott et al. 2000). There is no evidence for evolution of this ratio as a function of redshift.

The perceived picture of the optical appearance of high redshift radio galaxies is biased towards the most luminous objects (e.g. 3C radio galaxies) which have been most widely studied. High-redshift 3C radio galaxies have very strong high-ionization emission lines and tend to have blue optical-to-near-infrared colours due to extended rest-frame UV emission which is either non-stellar in origin or due to jet-triggered star-formation (e.g Best et al. 1998). Due to the correlation between emission line strengths and radio luminosity (Rawlings & Saunders 1991), lower luminosity radio galaxies have much weaker lines. They also have less rest-frame UV emission and a large fraction of them are classified as extremely red galaxies ($R - K > 5$) with colours typical of old galaxies at $z > 1$ (Willott et al. 2001).

The identification of hard Chandra sources with galaxies which are faint in the optical and very red (Giacconi et al. 2001; Crawford et al. 2000; Barger et al. 2001) suggests that many of these may also be evolved galaxies at $z > 1$. Cowie et al. (2001) present high quality data on a couple of such objects showing that they do indeed appear to be red galaxies with little contribution to the broad band magnitudes by AGN emission. Although such objects do not always show strong narrow emission lines, their high redshifts imply high X-ray luminosities

for samples with flux-limits similar to the ELAIS Chandra observations. Accounting for the hard X-ray absorption, (which can be a factor of 10 for Type 2 quasars detected at 2-10 keV; Norman et al. 2001) then the intrinsic luminosities would be very high and well above the $L_{2-10\text{keV}} > 10^{44}\text{erg cm}^{-2} \text{ s}^{-1}$ criterion. The large number of faint galaxy counterparts in Fig. 2 suggest that a sizeable fraction of ELAIS Chandra sources will be Type 2 quasars at $z > 1$.

We have obtained optical spectra from the WHT for a small sample of five hard X-ray selected ELAIS Chandra sources. Redshifts were determined for three of the five sources (the two undetected sources have $R \sim 25$ and very red optical to near-IR colours). Spectra of the three sources with emission lines are shown in Figure 4. Two sources have spectra which are very similar to those of high-redshift radio galaxies, with narrow ($\text{FWHM} < 1500 \text{ kms}^{-1}$) lines. CXON2_25 has slightly broader emission lines ($1800 - 2500 \text{ kms}^{-1}$) and is most likely a heavily reddened quasar. The X-ray luminosities of the two $z > 2$ X-ray sources are $L_{2-10\text{keV}} > 10^{44}\text{erg cm}^{-2} \text{ s}^{-1}$ and that of the $z = 1$ source is $> 10^{43}\text{erg cm}^{-2} \text{ s}^{-1}$. Accounting for the large absorption depression of the hard X-ray luminosity (all have $HR > 0$), all three sources are classified as Type 2 quasars. We expect that complete spectroscopic follow-up of the survey will lead to the discovery of many more such objects and determine their redshift distribution. Folding in the knowledge of the amount of absorption from the high quality X-ray spectra which will come from our deep XMM-Newton pointing, we will be able to derive the relative space densities of Type 2 to Type 1 sources and its dependence upon redshift and luminosity.

5 Studies of Type 2 quasar hosts

The large numbers of Type 2 quasars which will be identified in deep hard X-ray surveys provide a new opportunity to study the host galaxies of AGN, without the difficulties of PSF subtraction which complicate studies of Type 1 quasar hosts. The near-infrared Hubble diagram (or $K - z$ relation) of radio galaxies up to $z \sim 4$ is consistent with passive evolution of massive galaxies with luminosities in the range $2 - 5L_*$ (Jarvis et al. 2001). By comparing 3C radio galaxies with fainter samples (6CE, 7CRS) there is evidence for a weak correlation of stellar K -band luminosity with radio luminosity (Eales et al. 1997; Willott et al., in prep.). This correlation is likely to have its origins in the black hole mass – bulge mass – stellar velocity dispersion correlations (Magorrian et al. 1998; Gebhardt et al. 2000) since the K -band luminosity is a good indicator of the stellar mass.

In Figure 5 we show the near-infrared Hubble diagram for an incomplete sample of Chandra sources without broad emission lines (ELAIS Deep; Hornschemeier et al. 2001; Barger et al. 2001; Cowie et al. 2001). The X-ray sources have a wider range of K -band luminosities than the radio galaxies, from sub- L_* to $5L_*$. This can be explained in terms of the correlation found for radio galaxies mentioned above. The X-ray sources range from very low luminosity to powerful AGN and it is likely that powerful AGN only occur in the more massive galaxies which have large black holes. The sub- L_* host galaxies are generally at low redshifts, where the correlations between luminosity and redshift in the samples mean that they have low X-ray luminosities. However, it is worth remembering that these samples are nowhere near complete in terms of spectroscopic redshifts and obtaining redshifts for low-luminosity X-ray sources at $z > 1$ will be very difficult. Confirmation of this result will be possible when complete samples are available and emission line contributions to the magnitudes at K -band can be estimated.

References

1. Antonucci R.R.J., 1993, ARAA, 31, 473
2. Barger A., Cowie L.L., Mushotzky R.F., Richards E.A., 2001, AJ, 121, 662
3. Barthel P.D., 1989, ApJ, 336, 606

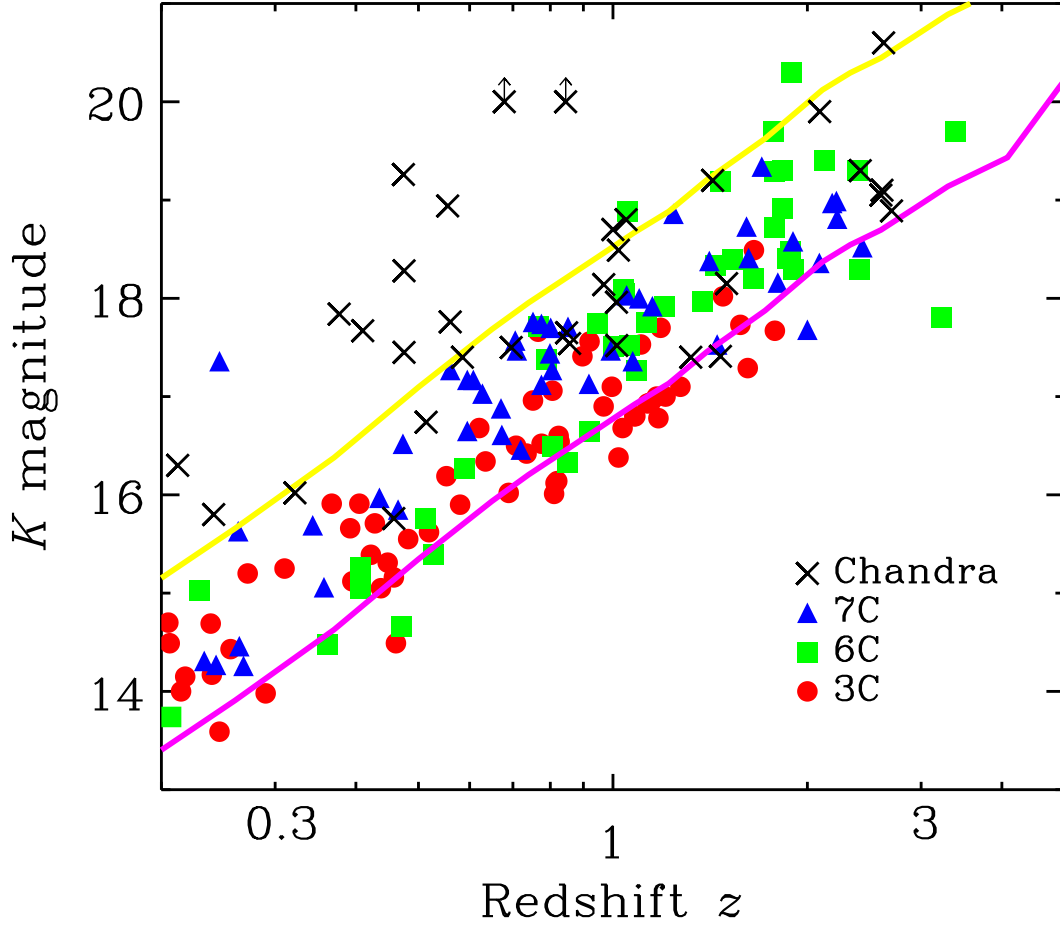


Figure 5: The near-infrared Hubble diagram for radio galaxies from the 3C, 6C and 7C samples and Type 2 X-ray sources from Chandra surveys. Note that the X-ray source host galaxies have a much larger range of K -band luminosities than the radio galaxies. The curves are passive evolution models for galaxies which formed all their stars in a short burst at high redshift ($z = 10$). The upper curve corresponds to L_* and the lower curve to $5L_*$

4. Best P.N., Longair M.S., Röttgering H.J.A., 1998, MNRAS, 295, 549
5. Ciliegi P., et al., 1999, MNRAS, 302, 222
6. Comastri A., Setti G., Zamorani G., Hasinger G., 1995, A&A, 296, 1
7. Cowie L.L., et al., 2001, ApJ, 551L, 9
8. Crawford C.S., Fabian A.C., Gandhi P., Wilman R.J., Johnstone R.M., 2000, MNRAS, submitted, astro-ph/0005242
9. Dunlop J.S., 2000, UMass/INAOE conference proceedings on 'Deep millimeter surveys', eds. J. Lowenthal and D. Hughes, World Scientific, astro-ph/0011077
10. Eales S.A., Rawlings S., Law-Green J.D.B., Cotter G., Lacy M., 1997, MNRAS, 291, 593
11. Giacconi R., et al., 2001, ApJ, 551, 624
12. Gebhardt K., et al., 2000, ApJ, 539, 13
13. Gilli R., Salvati M., Hasinger G., 2001, A&A, 366, 407
14. Gilli R., Risaliti G., Salvati M., 1999, AN, 320, 282
15. Halpern J.P., Turner T.J., George I.M., 1999, MNRAS, 307L, 47
16. Hasinger G., et al., in "Highlights in X-ray Astronomy", MPE report 272, p.199
17. Hornschemeier A.E., et al., 2001, in press, astro-ph/0101494
18. Jarvis M.J., et al., 2001, MNRAS, in press

19. Magorrian J. et al., 1998, *AJ*, 115, 2285
20. Maiolino R., et al., 2001, *A&A*, 365, 28
21. Norman C., et al., *ApJ*, submitted, astro-ph/0103198
22. Oliver S., et al., 2000, *MNRAS*, 316, 749
23. Rawlings S., Saunders R., 1991, *Nature*, 349, 138
24. Schreier E.J., et al., 2001, *ApJ*, in press, astro-ph/0105271
25. Sutherland W., Saunders W., 1992, *MNRAS*, 259, 413
26. Tozzi P., et al., 2001, *ApJ*, submitted, astro-ph/0103014
27. Willott C.J., Rawlings S., Blundell K.M., 2001, *MNRAS*, 324, 1
28. Willott C.J., Rawlings S., Blundell K.M., Lacy M., 2000, *MNRAS*, 316, 449